Visuohaptic Gross Shape Discrimination for 3D Watermarking

Kwangtaek Kim[1], Mauro Barni[2], Domenico Prattichizzo[2], and Hong Z. Tan[1],

[1] Haptic Interface Research Lab, School of Electrical **and** Computer Engineering
Purdue University, West Lafayette, IN, USA
{samuelkim, hongtan}@purdue.edu.
[2] Department of Information Engineering,
University of Siena, via Roma 56, 53100, Siena, Italy
{barni, prattichizzo}@dii.unisi.it

Abstract. With the advance of virtual reality and haptic technologies, watermarking of 3D visuohaptic contents is a new field to be developed in preparation of the need to protect those contents. Until now, there was no watermarking method developed in this field. In order to develop a new watermarking method for the visuohaptic contents, the study of human perceptibility of watermarking should be conducted as a preliminary work for embedding imperceptible watermarks into the contents. We therefore studied human perceptibility to gross shape changes because the gross shape of 3D objects can be used as a primitive for 3D visuohaptic watermarking. For our study, we designed and conducted psychophysical experiments in order to investigate human perceptibility on three types of gross-shape deformations (compressing, stretching and shearing) with two basic shapes (sphere and cube) over three conditions (Vision(V), Touch(T) and both (VH)). The result showed that vision was dominant and more sensitive than touch to gross shape changes no matter what type of shapes. The results suggest that the human sensitivity over different modalities should be carefully taken into account when we develop watermarking schemes employing the gross shape property of visuohaptic contents.

1 Introduction

Watermarking of 3D objects is receiving more and more attentions due to the increasing importance that 3D objects are getting in a wide variety of applications [1,2,3,4,5,6,7,9,10,11]. Technological advances have made it possible for fast and realistic rendering of 3D objects, thus encouraging their use in the creation of realistic virtual environments. With the increased diffusion, the need to protect 3D objects from misuse increases as well, hence raising the interest in 3D watermarking technology. A well known aspect of digital watermarking is the need to embed watermarks in such a way that the introduced degradation is not perceivable. Such a need has prompted a few studies addressing the problem of watermark visibility when a 3D object is rendered through common computer graphics techniques [8].

With the introduction of force-feedback devices that allow kinesthetic interaction with virtual environments, users will also be able to feel the virtual objects and enjoy an increased sense of presence inside simulated scenarios. In these applications, 3D digital models are perceived not only through the visual system, but also haptically. It is evident that for this kind of applications, it is necessary that the distortion introduced by the watermarking process does not disturb the haptic interaction with the 3D objects, i.e. the watermark must also be haptically imperceptible.

Previous studies [17,15,16] have investigated watermark perceptibility from an haptic point of view, reaching the conclusion that, at least under some conditions, the presence of the watermark is more easily detected by means of an haptic interface rather than through vision. A characteristic of the experiments underlying the works carried out so far is the *highpass* nature of the watermark, often consisting of a white pseudo-noise sequence. Though the degradation introduced by the watermark strongly depends on the particular embedding strategy, this kind of watermarks always result in a modification of surface details of the 3D mesh, which is often perceivable as an increased surface roughness. It is such an increased roughness that makes the watermark presence easily perceivable when the 3D object is sensed through an haptic interface.

It is arguable that this will not be the case if the watermark is embedded in such a way that only *gross shape* of the object is changed while leaving its surface details intact, e.g. leaving the smoothness of the surface intact. In this framework, the scope of our research is to investigate the perceptibility of the deformation of the gross shape of a 3D object from a visual and a haptic point of view. Our study may be seen as a further step towards the design of a haptically aware watermarking system in which haptic imperceptibility is taken into account along with watermark invisibility.

For our study, three types of deformations (compressing, shearing, and stretching) of 3D gross shapes were chosen, and a simulator was developed to create those deformations in a PC environment. With the developed simulator, a psychophysical experiment has been designed and conducted to investigate discrimination thresholds with two basic shapes (sphere and cube) over three conditions (Visual(V), Touch(T), and both (VH)). The results show that vision is not only dominant but also more sensitive than touch in terms of perceiving deformations of 3D objects. Next we describe the theory of 3D gross shape deformation and its simulation in Section 2, and then present the pychophysical experiment with its results in Section 3. In Section 4, we conclude this article with discussion.

2 3D Gross Shape Deformations With Simulations

As our point of view to represent a 3D object, two terms are defined: *gross shape* and *surface details*. The *gross shape* represents the global rough shape of an object while the *surface details* include small geometrical changes and texture on the surface of the object. For instance, when we look at a basketball, the *gross shape* is a sphere, and the *surface details* are the black ribs and rubber texture.

With these definitions, all 3D objects can be represented how they look like. For our study, we use the definition of *gross shape*. In the rest of this section, we describe how we developed three linear transformations to manipulate 3D gross shapes and a virtual simulator that interfaces with a PC and a haptic device for our perception study.

2.1 Three Linear Deformations: compressing, shearing, and stretching

Among all the possible deformations of the shape of a 3D object, we focused on the more common types of compressing, shearing, and stretching. These deformations of the shape of 3D objects can be modeled with affine transformations. In what follows, we will define the three types of geometrical manipulations of 3D objects described by polygonal meshes:

compressing makes the gross shape of an object more compact by pressing.
shearing deforms the gross shape in which parallel planes remain parallel but are shifted in a direction parallel to themselves.
stretching makes the shape of an object longer.

The three deformations are illustrated in Figure 1 to familiarize readers about them with a cube as an example. Specifically, compressing (see Figure 1(a)) changes side lengths αs of the top to βs with the same increment. Shearing (see Figure 1(b)), by a force applied to an object perpendicular to a given axis with a greater value on one side than the other of the axis, changes the height α to β but keeps side lengths αs of the top the same. By stretching (see Figure 1(c)), side lengths αs of the side face are decreased to βs with the same amount but the width α is increased to γ (see Figure 1(c)). These three basic manipulations provide different ways to change the gross shape of a 3D object.

In order to formularize the 3D linear transformations, an equation is introduced as $S_{new} = T(S_{old})$ where S_{new} and S_{old} are polygonal surfaces, and T denotes a linear function that transforms S_{old} into S_{new} for one of the three deformations. The linear function T can be set up as a four-by-four matrix for non-homogeneous 3D coordinates [x, y, z, 1] as the matrix shown below ($T_{4\times4}$) that looks like an affine transformation matrix without translation.

After an analysis of the matrix $T_{4\times4}$, it was found that (1) parameters a, e, and h play a role in compressing and stretching, and (2) the other parameters (b, c, d, f, g, and i) cause shearing of 3D shape. Additionally, all entries in the matrix are symmetry with respect to an axis, which minimizes the number of parameters for symmetric 3D objects. With these facts, two matrices with one parameter each are built for the three deformations as the T_1 and T_2 matrices shown below. Note that T_1 works for both compressing and stretching, while T_2 works for shearing.

$$T_{4\times4} = \begin{bmatrix} a & b & c & 0 \\ d & e & f & 0 \\ g & h & i & 0 \\ 0 & 0 & 0 & 1 \end{bmatrix}, T_1 = \begin{bmatrix} a & 0 & 0 & 0 \\ 0 & 1 & 0 & 0 \\ 0 & 0 & 1 & 0 \\ 0 & 0 & 0 & 1 \end{bmatrix}, \text{and } T_2 = \begin{bmatrix} 1 & b & 0 & 0 \\ 0 & 1 & 0 & 0 \\ 0 & 0 & 1 & 0 \\ 0 & 0 & 0 & 1 \end{bmatrix}$$

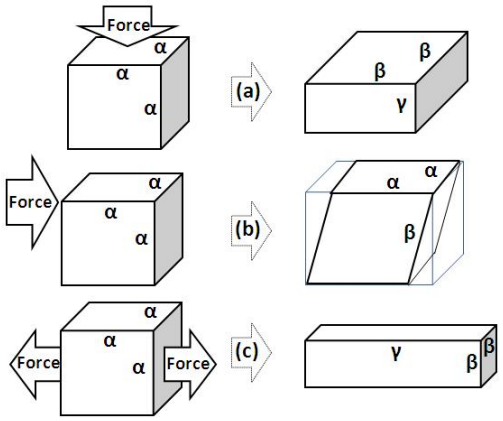

Fig. 1: Three geometrical deformations: compressing, shearing, and stretching. α, β and γ denote side lengths.

Volume-invariant Transformations Of the matrices derived above, T_1 is not volume-invariant, i.e., the object's volume changes during the deformations. For our study, we wanted to focus on 3D shape deformations without scaling in order to make it more realistic. Imagine creating a shape with a play-dough, the volume of the play-dough is preserved no matter what external forces are applied. In order to achieve this goal, we derived new matrices that preserve the volume for all deformations. To achieve volume invariance, two matrices are derived from matrix T_1, and matrix T_2 is rewritten with γ as shown below. In this way, three matrices are set up for the three deformations (compressing, shearing, and stretching) used in our perception study.

$$T_{compress} = \begin{bmatrix} \gamma & 0 & 0 & 0 \\ 0 & \frac{1}{\gamma^2} & 0 & 0 \\ 0 & 0 & \frac{1}{\gamma} & 0 \\ 0 & 0 & 0 & 1 \end{bmatrix}, T_{stretch} = \begin{bmatrix} \gamma & 0 & 0 & 0 \\ 0 & \frac{1}{\sqrt{\gamma}} & 0 & 0 \\ 0 & 0 & \frac{1}{\sqrt{\gamma}} & 0 \\ 0 & 0 & 0 & 1 \end{bmatrix}, T_{shear} = \begin{bmatrix} 1 & \gamma & 0 & 0 \\ 0 & 1 & 0 & 0 \\ 0 & 0 & 1 & 0 \\ 0 & 0 & 0 & 1 \end{bmatrix} \quad (1)$$

2.2 Development of Simulator

For virtual simulations of gross shape changes, a simulator of the three deformations employing the matrices was developed with Visual C++, Chai3D and OpenGL libraries on a PC. Gouraud shading technique [14] was used for visual rendering, and for haptic rendering, Ruspini's force shading [13] that is built in to Chai3D library was used. With the matrices with parameter γ described above, three geometrical deformations (compressing, stretching, and shearing) were developed so that polygonal surface can be linearly transformed in a PC environment. Figure 2 shows examples of the three deformations simulated with our developed simulator with a Bunny model.

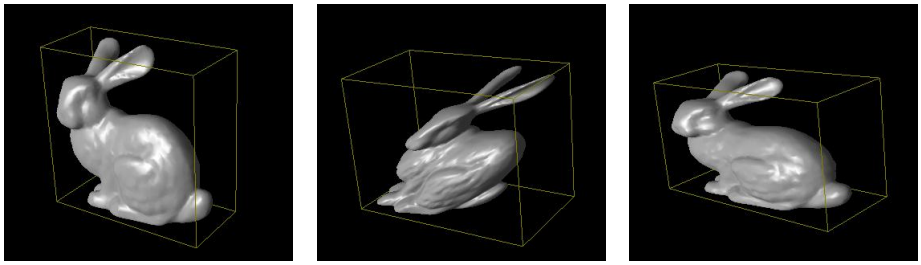

(a) Compressing with $\gamma = 1.2$ (b) Shearing with $\gamma = 1$ (c) Stretching with $\gamma = 1.5$

Fig. 2: Gross shape manipulations by our developed simulator with a Bunny model (not used in the present study).

3 Psychophysical Experiment

With our developed simulator, a psychophysical experiment was conducted to estimate discrimination thresholds on the three deformations (compressing, shearing and stretching) of 3D gross shapes over three conditions (Visual only (V), Haptic only (H), and both (VH)). In the rest of this section, we describe the experiment and present the results.

3.1 Participants

Four participants (3 males and 1 female, age range 22-36 years old, average age 27.8 years old) took part in the experiment. All participants were right-handed by self-report. Participants P2, P3, and P4 had previous experience with haptic interfaces and perception experiments. None of the participants reported any deficiencies in vision or touch.

3.2 Apparatus

To test the haptic modality, a custom-designed 3-DOF (degrees of freedom) force-feedback device, the "ministick" (see Figure 3), was used for the experiments. A user interacts with virtual 3D objects by stroking with a stylus magnetically connected to the end effector of the ministick. A standard LCD 19" PC monitor (1280 by 1024 pixels) was used for the visual display, and a keyboard was used by the participant to enter his/her response.

3.3 Stimuli

Two 3D shapes as seen in Figure 4, cube and sphere, were created with 3DS Max software and were presented as stimuli to the participants through visual and haptic interfaces. The test stimulus was presented after compressing, shearing, or stretching transformation controlled by the value of γ , a parameter of the

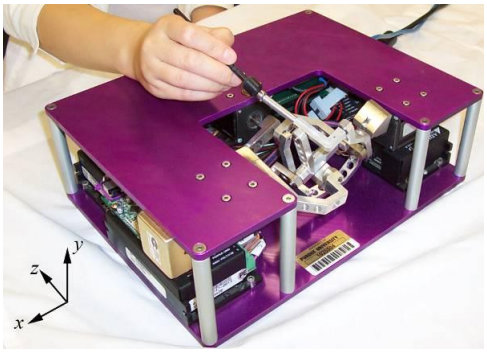

Fig. 3: The ministick

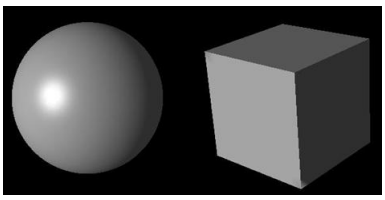

Fig. 4: Stimuli: cube and sphere

matrices $T_{compress}$, $T_{stretch}$ and T_{shear}, from Eqn. 1. During the experiment, δ was increased or decreased from trial to trial. For the experiment, the δ values for the reference stimulus (γ_{ref}) were 1.1 for both compressing and stretching, and 0.1 for shearing, respectively.

3.4 Procedures

A three-interval forced choice (3IFC) one-up three-down adaptive procedure [12] was used to estimate discrimination thresholds of gross shape changes over three conditions (V, H, and VH). On each trial, for the V (H) condition, the participant looked at (touched) sphere or cube presented through the monitor (the ministick), respectively. For the VH condition, the participant looked at as well as touched sphere or cube by interfacing with both the monitor and the ministick. One of three stimuli had a deformed shape with the strength specified by δ_{test}. The participant's task was to indicate which shape looked and/or felt different. The orientation of the shape was randomly chosen on each trial, but the participant was able to rotate the stimulus any time with the mouse interface. An alignment function with respect to x axis was also provided when the participant pressed a reset key during the experiment. By doing this, the difficulty of perception caused by randomized orientation between the V and H conditions was balanced.

According to the one-up three-down adaptive rule, the value of δ_{test} was increased after a single incorrect response and decreased after three successive

correct responses; otherwise, the value of δ_{test} remained the same. The initial δ_{test} value was chosen to be large enough so that the gross shape change was clearly perceptible to the participant. The value of δ_{test} then decreased or increased by 6 dB, depending on the participant's responses. After the initial three reversals (a reversal occurred when the value of δ_{test} decreased after an increase, or vice versa), the value of δ_{test} changed by 2 dB. The initial larger change in δ_{test} was necessary for a fast convergence of the δ_{test} values, whereas the later smaller change in δ_{test} improved the resolution of threshold estimates. The adaptive series was terminated after 8 reversals at the smaller step size. The discrimination threshold was computed by taking the average of the δ_{test} value from the last 8 reversals. The participants were comfortably seated before a computer screen, the ministick, and a keyboard. Initial training was provided where a series of stimuli were presented to familiarize the participants with the three types of deformations and experimental conditions. Each participant was tested once per deformation type, shape, and conditions, resulting in a total of eighteen adaptive series per participant.

3.5 Data Analysis

For each adaptive series, thresholds were calculated as $\delta_{test} - \delta_{ref}$ from the peak and valley δ_{test} values over the last eight reversals at the 2 dB step size. Specifically, four threshold values were estimated by averaging the four pairs of peak/valley amplitude values recorded during the last 8 reversals. The mean and the standard deviation for the discrimination thresholds were then calculated from the four threshold estimates. According to Levitt [12], the resulting thresholds converged on the psychometric function at the 79.4 percentile level.

3.6 Experimental Results

Figure 5 shows the results of the psychophysical experiment that we have conducted above. On the plot, bar graphs represent the averaged thresholds of all participants, and the error bars are standard deviations. Note that there is no unit on the vertical axis on the chart since the thresholds are scaling factors. The thresholds of the H condition were significantly larger than those of the other two conditions over all three types of deformations. This was true for both cube and sphere shapes (see Figure 5(a) and 5(b), respectively). It was also apparent that the thresholds for the V and VH conditions were almost identical regardless of the type of shapes or deformations.

A closer examination of Figure 5reveals that variation of the thresholds with the H condition was larger than that of the thresholds with the other two conditions (V and VH) over all three deformations and the two shapes. The smallest and largest thresholds were compressing and shearing with cube, and compressing and stretching with sphere. When the thresholds are compared between the two shapes, the thresholds for the V and VH conditions with the cube were slightly larger than these with sphere for both stretching and compressing.

In order to investigate the significance of interactions between two factors (conditions and deformations), the results were tested with a two-way ANOVA. It was found that both factors significantly affected the results with the sphere shape [conditions:$F(2,28)=28.69$, $p<0.0001$; deformation: $F(2,28)=3.46$, $p=0.0453$], For the cube shape, only the condition factor was significant [conditions: $F(2,28)=23.81$, $p<0.0001$; deformations: $F(2,28)=2.80$, $p=0.0778$]. A contrast test was conducted to check whether there was significant difference among the conditions. It confirmed that there was no significant difference between the V and VH conditions over all three deformations with both shapes, but there was a significant difference between two groups (H) vs. (V and VH) with both shapes [$p<0.0001$]. It also confirmed that the thresholds of compressing were significantly different (smaller) from those of the other two deformations with only the sphere [$p=0.0280$,0.0332], and there was also a significant difference between the two groups (compressing) vs. (stretching and shearing) for the H condition with both shapes [cube:$p=0.0084$; sphere:$p=0.0329$].

4 Discussion

We have studied the human visual and/or haptic sensibility to three type of gross shape deformations (compressing, shearing and stretching) with two shapes (cube and sphere). For both shapes, we found that vision was dominant since the thresholds of V and VH conditions were almost identical, while touch was less sensitive than vision in perceiving the gross-shape change of a 3D object regardless of the type of deformation.

Another finding was that discriminating compressed gross shapes was the easiest task especially for the haptic condition. It makes sense when consider the most interested area where the participants largely focus on stroking the haptic device to make a decision. For instance, to compare between the test and reference stimuli, the participants had the narrower area for compressing than for the other two deformations. In other words, human become less sensitive in the haptic channel as the range of area to be explored increases.

Our study complements the initial studies on haptic watermark presented in [15,16,17] where the authors showed that the haptic modality was more sensitive when the vertices of 3D polygonal meshes were altered by additive random noises. Studies in papers [15,16,17] achieve shape changes though vertex perturbations, thus resulting in more local changes when compared to the study presented here. Our result that vision is more sensitive to changes of the gross shape is to be expected since the vision modality is better able to capture global information like the shape when compared to haptic interaction with a single contact point. Interacting with a stylus allows us to perceive only a very small local part of the 3D shape which does not allow us to get the whole shape. We suppose that with more advanced haptic interaction devices that one easily able to simulate the grasp of an object; a multi-finger and palm interactions, haptic perception threshold may become comparable with the vision threshold.

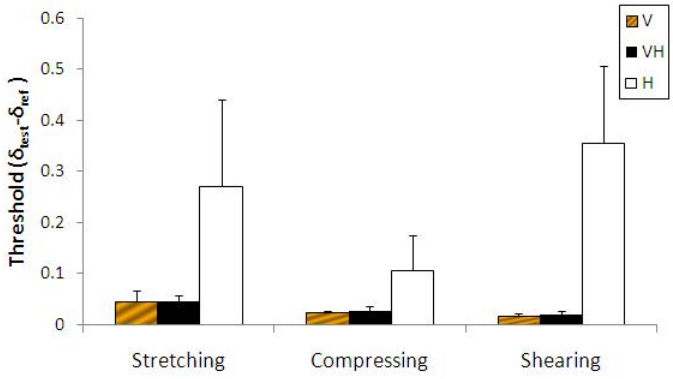

(a) Cube

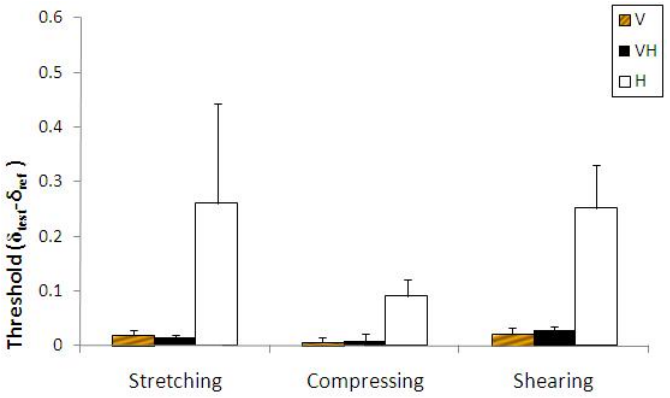

(b) Sphere

Fig. 5: Averaged thresholds with two shapes. Error bars are standard Dev.

For future work, we plan to investigate how current shading techniques for both haptic and visual channels affect human perceptibility where changing the high frequency components of visuohaptic contents. We must carefully examine the effect of shading on human perceptibility since using shading technologies for watermarking is a natural way to display 3D digital contents, and our initial studies by now did not take into account force shading technologies. We will then develop haptic-aware watermarking algorithms that employ the results of our perception studies for visuohaptic contents that are altered in both gross shapes and surface roughness.

Acknowledgments

The first and last authors (KK and HZT) were partially supported by the US National Science Foundation under Grant no. 0836664. The second author (MB) was partially supported by the Italian Ministry of Research and Education under FIRB project no. RBIN04AC9W.

References

1. R. Ohbuchi, H. Masuda, and M. Aono, "Watermarking three-dimensional Polygonal Models", in Proceeding of the fifth ACM international conference on Multimedia. Siattle, Washington, United States: ACM, 1997, pp. 261-272.
2. O. Benedens, "Geometry-based watermarking of 3d models", Computer Graphics and Applications, IEEE, vol. 19, no. 1, pp. 46-55, 1999.
3. Z. Karni and C. Gotsman, "Spectral compression of mesh geometry", in SIGGRAPH '00: Proceedings of the 27th annual conference on Computer graphics and interactive techniques, 2000, pp. 279-286.
4. F. Cayre and B. Macq, "Data hiding on 3-d triangle meshes", IEEE transactions on Signal Processing, vol 51, no. 4, pp. 939-949, 2003.
5. F. Ucceddu, M. Corsini, and M. Barni, "Wavelet-based blind watermarking of 3d models", in MM&Sec 2004: Proceedings of the 2004 workshop on Multimedia and security. ACM, 2004, pp. 143-154.
6. S. Zafeiriou, A. Tefas, and I. Pitas, "Blind robust watermarking schemes for copyright protection of 3d mesh objects", IEEE Transactions on Visualization and Computer Graphics, vol. 11, no. 5, pp. 596-607, 2005.
7. A. Bors, "Watermarking mesh-based representations of 3-d objects using local moments", IEEE transactions on Image Processing, vol. 15, no. 3, pp. 687-701, 2006.
8. M. Corsini, E. D. Gelasca, T. Ebrahimi, and M. Barni, "Watermarked 3-d mesh quality assessment", IEEE Transactions on Multimedia, vol. 9, no. 2, pp. 247-256, 2007.
9. K. Wang, G. Lavoue, F. Denis, and A. Baskurt, "Hierarchical watermarking of semiregular meshes based on wavelet transform", IEEE Transactions on Information Forensics and Security, vol. 3, no. 4, pp. 620-634, Dec 2008.
10. K. Kim, M. Barni, and H. Z. Tan, "Roughness-adaptive 3d watermarking of polygonal meshes", Information Hiding: 11th International Workshop, pp. 191-205, Darmstadt, Germany, June 8-10, 2009.
11. J. Konstantinides, A. Mademlis, P. Daras, P. Mitkas, and M. Strintzis, "Blind robust 3-d mesh watermarking based on oblate spheroidal harmonics", IEEE Transactions on Multimedia, vol. 11, no. 1, pp. 23-38, Jan. 2009.

12. H. Levitt, "Transformed up-down methods in psychoacoustics," Journal of the Acoustical Society of America, vol. 49, pp. 467-477, 1971.
13. Diego. C. Ruspini, Krasimir Kolarov, and Oussama Khatib, "The haptic display of complex graphical environments", In SIGGRAPH 97 Conference Proceedings, pages 345-352, August 1997.
14. H. Gouraud "Continuous Shading of Curved Surfaces." IEEE Transactions on Computers, C-20(6): pp 623-629, June 1971.
15. Domenico Prattichizzo, Mauro Barni, Hong Z. Tan, and Seungmoon Choi, "Perceptibility of haptic digital watermarking of virtual textures", Proceedings of the 2005 World Haptics Conference, The First Joint Eurohaptics Conference and Symposium on Haptic Interfaces for Virtual Environment and Teleoperator Systems, Pisa, Italy, pp. 50-55, Mar. 18-20, 2005.
16. Alessandro Formaglio, Sara Belloni, Gloria Menegaz, Hong Z. Tan, Domenico Prattichizzo, and Mauro Barni, Perceptibility of digital watermarking in haptically enabled 3D meshes, Proceedings of Eurohaptics Conference 2006, Paris, France, pp 407-412, July 3-6, 2006.
17. Domenico Prattichizzo, Mauro Barni, Gloria Menegaz, Alessandro Formaglio, Hong Z. Tan, and Seungmoon Choi, "Perceptual issues in haptic digital watermarking", IEEE Multimedia, Vol. 14, No. 3, pp. 84-91, 2007